

# Calculation of the effects of protonation on rigid-rod polymers

B. L. Farmer\*

Department of Materials Science and Engineering, University of Virginia, Charlottesville, VA 22093-2442, USA

and D. S. Dudis† and W. W. Adams‡

Wright Laboratory, Materials Directorate, † WL/MLBP and ‡ WL/MLPJ, WPAFB, OH 45433, USA

(Received 21 July 1993; revised 4 January 1994)

Semiempirical molecular orbital calculations have been used to investigate the effects of protonation on the behaviour of the structural repeat units of poly(*p*-phenylene benzobisthiazole), PBZT, and poly(*p*-phenylene benzobisoxazole), PBO. Single and multiple protonations of the heterocyclic rings at the nitrogen, oxygen and/or sulfur atoms were examined. It was found that protonation at the nitrogen was more favourable than at the oxygen or sulfur atoms. Delocalization of the charge into the phenyl ring resulted in a higher bond order for the inter-ring bond. While the energy barrier for torsional rotation increased with protonation, the resistance to bending the rings in an out-of-plane fashion decreased somewhat. Results of the semiempirical calculations indicated that protonation of the oxygen in PBO might result in opening of the five-membered heterocyclic ring by breaking the carbon–oxygen bond. *Ab initio* calculations on relevant models, however, did not support this result.

(Keywords: protonation; rigid-rod polymers; semiempirical calculations)

## INTRODUCTION

Experimental measurements of the persistence lengths of rigid-rod polymers in solution, although complicated by effects of aggregation, yield values of the contour length substantially less than would be expected for an extended molecule having the molecular weight measured for the polymer<sup>1,2</sup>. Molecular dynamics (MD) calculations<sup>3–5</sup> have been used to examine rigid-rod polymers in an effort to understand the flexibility implied by their measured persistence lengths. Calculations<sup>3,4</sup> modelling isolated polymer chains *in vacuo* give values of the persistence lengths even shorter than the observed values. Investigation<sup>3</sup> of the force field used in those MD simulations suggests that the observed flexibility may indeed be an underestimation of the actual situation, and that the experimentally observed values are as high as they are because of aggregation effects. (Other MD simulations using a stiffer force field give persistence lengths comparable with the observed values<sup>5</sup>.) Simulations of an assembly of rigid-rod molecules (approximating a crystalline environment) also show substantial (though much less than observed *in vacuo*) deviations from strict rigidity and linearity<sup>6–8</sup>.

Apart from questions of the most appropriate force field, the simulations thus far have not realistically addressed the behaviour of the polymer in a solvent, nor the effects of aggregation. Placing a rigid-rod polymer in a normal solvent would not be expected to have much impact on its stiffness. However, for experimental

measurements, the rigid-rod polymers are generally dissolved in strong protonating acids, where protonation of the polymer molecule is not only very likely, but is probably a precondition to dissolution. (Rigid-rod polymers complexed with Lewis acids, however, do dissolve in aprotic organic solvents<sup>9</sup>.) Protonation may introduce two effects that might tend to stiffen the polymer. By virtue of the positive charges on the chain, repulsive Coulombic interactions between adjacent heterocycles may tend to extend and stiffen the chain. Shielding effects of the counterions and the strong acid medium, on the other hand, may greatly diminish this effect. Another possibility is that protonation may affect (and increase) the force constants which dictate the vibration and deformation behaviour of the molecule. This latter effect is addressed in this paper.

## METHOD

The calculations were performed using the AM1 Hamiltonian in MOPAC<sup>10</sup>, Version 5. Modified neglect of differential overlap (MNDO) parameters were used to describe the sulfur atoms. Default minimization procedures and optimization criteria were used. The model molecules, shown in *Figure 1*, represent one repeat unit of *cis*-PBO or *trans*-PBZT capped with hydrogen atoms at the *para* positions. These particular isomers were of interest because of the potential technological value arising from their outstanding mechanical properties<sup>11,12</sup>. The starting geometries for the molecular orbital calculations were the structures

\*To whom correspondence should be addressed

determined by a molecular mechanics minimization using Sybyl<sup>13</sup> and a version of the Tripos force field<sup>14</sup> modified<sup>3</sup> to give agreement with previous AM1 results<sup>15</sup> on the neutral molecules. MOPAC energy minimizations were carried out with full geometry optimization (except as noted below). Protons (and a charge of +1

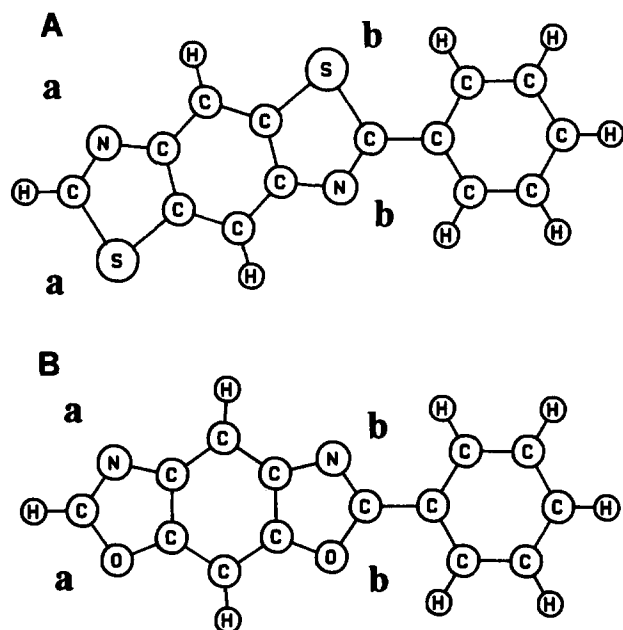


**Figure 1** Schematic diagram of the structures of PBZT (A) and PBO (B) used in the calculations, and showing the designations of the protonation sites

**Table 1** Energies associated with protonating the heterocycles of PBO and PBZT at various positions

		Heat of formation (kcal mol <sup>-1</sup> )	Bond order (inter-ring bond)
<b>PBO (torsion = 0)</b>			
Neutral		67.98	1.00
1 hydrogen (+1)	N <sub>a</sub>	223.03	1.02
	N <sub>b</sub>	216.78	1.06
	O <sub>a</sub>	228.60	(ring opening)
	O <sub>b</sub>	219.17	(ring opening)
Radical cation +1		262.90	1.18
2 hydrogens (+2)	N <sub>a</sub> , N <sub>b</sub>	438.87	1.16
	N <sub>b</sub> , O <sub>b</sub>	515.88	1.22
3 hydrogens (+3)	N, N, O <sub>a</sub>	818.41	1.34
	N, N, O <sub>b</sub>	802.75	1.44
Radical cation +2		539.85	1.51
4 hydrogens (+4)		1245.56	1.62
<b>PBZT (torsion = 0)</b>			
Neutral		130.37	1.01
1 hydrogen (+1)	N <sub>a</sub>	283.24	1.03
	N <sub>b</sub>	277.21	1.08
	S <sub>a</sub>	318.00	1.03
	S <sub>b</sub>	314.61	1.02
Radical cation +1		324.66	1.16
2 hydrogens (+2)	N <sub>a</sub> , N <sub>b</sub>	494.34	1.18
	N <sub>b</sub> , S <sub>b</sub>	557.97	1.24
Radical cation +2		594.25	1.45
		594.25	1.45
3 hydrogens (+3)	N, N, S <sub>a</sub>	853.28	1.35
	N, N, S <sub>b</sub>	838.94	1.35
4 hydrogens (+4)		1258.46	1.63

for each) were placed on the nitrogen, oxygen and sulfur atoms of the heterocycles individually and in various combinations. For identification and discussion purposes, the protonated atoms will be labelled with subscripts a and b (as shown in *Figure 1*) and referred to as 'exterior' and 'interior', respectively. Counterions were not included in the calculations.

Preliminary calculations for protonated PBZT began with a tetrahedral geometry for the protonated nitrogen atom. Starting torsions of 0 to 20° about the backbone single bond were examined, the latter being the minimum energy value for the neutral molecule<sup>3,16,17</sup>. Geometry optimization resulted in planar nitrogens with the proton in the plane of the heterocycle. The minimum energy torsion angle was 0°. Subsequent starting geometries for both PBO and PBZT thus assumed planar nitrogen atoms, an in-plane position for the proton, and a coplanar (0° torsion angle) conformation of the molecules.

*Ab initio* calculations were made using Gaussian 88<sup>18</sup>. The energies and optimized geometries were calculated for oxazole, corresponding to a five-membered ring fragment of the benzobisoxazole. Energies were calculated for some fragments at the RHF/3-21G\*, RHF/6-31G\*\* and MP2/6-31G\*\*. The RHF/3-21G\* level was used to explore fragments relevant to PBZT. The optimized geometries were consistently planar for both oxazole and thiazole, confirming the AM1 results and the planarity of the nitrogen atoms in the protonated species.

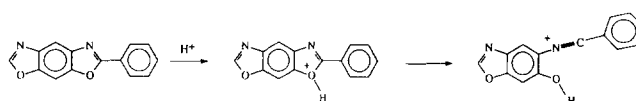
## RESULTS

### Protonation of PBO and PBZT

*Table 1* shows the energies associated with protonating the heterocycles of PBO and PBZT repeat units at various positions. Note that the model molecule has only one phenyl group, and that protonation has different effects depending upon which end of the heterocycle is involved. From the polymer viewpoint, this distinction is not relevant, but the model does show the effects of delocalization (and possibly polarization) between the phenyl and heterocyclic rings and the extra stabilization gained therefrom. The bond order of the inter-ring bond is also shown in the table.

For singly protonated PBO the energy was lowest for protonation at N<sub>b</sub>, where more delocalization of the charge is possible because of its proximity to the phenyl ring. Protonation at the other nitrogen atom was about 6 kcal mol<sup>-1</sup> higher. The same was true for the protonation of PBZT at each of the nitrogen atoms.

Protonation at the sulfur atoms in PBZT was 37 kcal mol<sup>-1</sup> higher in energy than protonation at the nitrogens. Again proximity to the phenyl group was advantageous. For PBO, protonation at the oxygen atoms was higher in energy than at the nitrogens, but only by 3 kcal mol<sup>-1</sup> when near the phenyl ring. More importantly, the AM1 results show that such protonation leads to opening the five-membered ring, described by *Scheme 1*. This observation was explored further using *ab initio* methods, as described below.



**Scheme 1**

Multiple protonations were also examined. Protonation at both nitrogen atoms was greatly favoured over protonation of the nitrogen and oxygen atoms of the same ring in PBO. By having the charges separated in this way, the Coulombic repulsions would be minimized. Interestingly, the latter multiple protonation did not lead to ring opening. Protonation of both nitrogens was likewise more favourable for PBZT than protonation of the nitrogen and sulfur atoms. In triple protonation, the influence of delocalization persisted in making the interior sulfur or oxygen more susceptible than the exterior ones.

Since these calculations were carried out without the presence of counterions, the overall energies for the protonated molecules increased dramatically. Taking the lowest energy for each successive level of protonation, the incremental energy for placing each additional proton likewise increased. For PBO, this *incremental* energy was found to be 149, 222, 364 and 443 kcal mol<sup>-1</sup> in going from the neutral to the quadruply protonated molecule in the order N<sub>a</sub>, N<sub>b</sub>, O<sub>b</sub>, O<sub>a</sub>. Values for PBZT were 147, 217, 345 and 420 kcal mol<sup>-1</sup>. In a similar fashion, each successive protonation increased the inter-ring bond order by increasing amounts.

The possibility of electron abstraction from the PBO and PBZT repeat units was also examined. Radical cations having charges of +1 or +2 were found to be higher in energy than the like-charged protonated species. These energy values are also presented in *Table 1*. The radical cations resulted in higher bond orders than did protonation at the same net charge.

#### Torsions and bond orders

Energy barriers to torsion about the inter-ring single bond for the neutral, singly and doubly protonated molecules were calculated with full geometry optimization, but of course with the inter-ring torsion fixed at the desired value. Ten degree increments were used in the unique range from 0 to 90°. Calculations of the barriers for higher protonation levels were not carried out because of the increasingly higher energy cost of such protonations and the increasingly serious consequences of neglecting solvent effects.

To determine the influence of starting geometry on the final minimized structure, the torsion angle *versus* energy curve for the diprotonated molecules was computed in two different ways: (1) the minimized 0° geometry – except for the inter-ring torsion which was set and fixed at the desired value – was used as the starting point; or (2) the optimum geometry computed for the previous torsion angle was used as the starting point for the optimization for the next value of the torsion angle. This latter sequential process is the same as used in previous calculations<sup>15–17</sup>. The minimizations which began with the 0° geometry consistently resulted in slightly lower energies. The values differed by no more than 1 kcal mol<sup>-1</sup>, however, which amounts to less than 0.2% of the calculated heat of fusion. The energy *versus* torsion angle curves differed most in the range 50–70°, while the energy barriers (at 90°) were very similar for both minimization methods. The curves reported here show the lower energy values.

*Figure 2a* shows the energy *versus* torsion angle for the neutral PBZT repeat unit and the protonated molecules having charges of +1 and +2. Energy values are shown relative to the energy calculated for each molecule at 0° torsion. Protonation shifts the energy

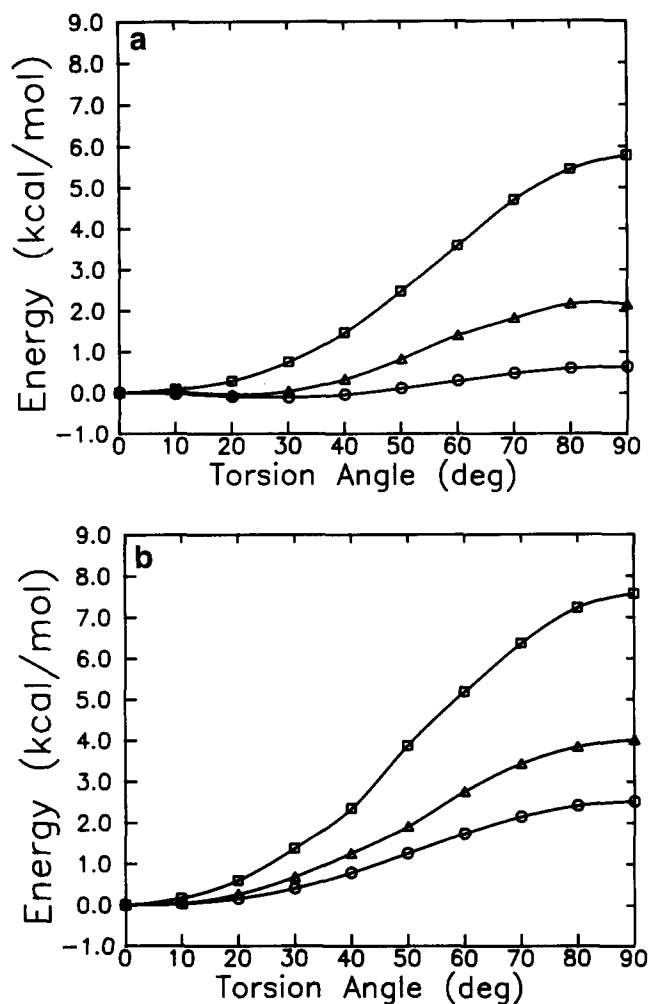


**Figure 2** Energy *versus* torsion angle for (○) neutral, (△) singly and (□) doubly protonated PBZT (a) and PBO (b). Protonation was at N<sub>b</sub> on the singly protonated molecules and at N<sub>a</sub> and N<sub>b</sub> for the doubly protonated

minimum to 0° (compared with about 30° for the neutral molecule) and raises the relative energy at 90° compared with the unprotonated, uncharged molecule. As shown in *Figure 2b*, a similar effect is seen for protonated PBO. The energy barriers are considerably smaller than CNDO/2 values previously reported<sup>19</sup>.

The cause of the dramatic change in the nature of the energy associated with rotation about the inter-ring single bond can be seen in *Figure 3* which shows the calculated bond order for this bond as a function of torsion angle. While the bond order at 0° torsion in unprotonated PBZT is 1.01, in diprotonated PBZT the bond order increases to 1.18. Similarly for PBO, the bond order in the neutral molecule at 0° torsion is 1.00, while the diprotonated molecule has a bond order of 1.16. For PBO and PBZT at 90° torsion, whether neutral or diprotonated, the bond order decreases to the range 0.97 to 0.99. In general, the changes in bond order might be attributed to either delocalization or polarization effects. However, polarization effects would not be affected by changes in torsion angle. Thus, as the rings are rotated from coplanarity, the loss of delocalization is the main contribution to the dramatically larger torsional energy barrier in the diprotonated molecule.

This effect can also be seen in the length of the inter-ring bond. In the diprotonated molecule, the bond length

increases from 1.424 Å at 0° to 1.449 Å at 90°, while in neutral PBZT the change is only slight (from 1.457 Å to 1.461 Å). Similar changes were observed in PBO.

The change in delocalization with bond rotation can also be seen in the distribution of charge among the atoms of the molecules. Figures 4 and 5 show comparisons of the atomic charges calculated by MOPAC for neutral PBZT and PBO and for diprotonated molecules having torsion angles of 0 and 90°. (The charge distribution did not change dramatically with torsion angle in the neutral molecules, so only the 0° values are shown.) It can be seen that the charge distribution in the diprotonated molecules with a 0° torsion is shifted toward the phenyl ring. Summing the partial charges on the atoms of the phenyl ring for the diprotonated molecules indicates that about 19–21% of the total charge resides on the phenyl ring. At 90° torsion, this drops to about 11%. The charge distribution in the neutral, coplanar molecule leaves the

phenyl ring slightly positive, with a total partial charge of about 0.10–0.13 esu on the phenyl ring. This decreases by only about 5% as the torsion angle changes from 0 to 90°.

#### Bending deformations

The results<sup>3,6-8</sup> of MD simulations of isolated molecules of PBO, PBZT and PPP and in a crystalline environment showed the molecules to be surprisingly flexible in spite of their rod-like topologies. The soft deformation mode responsible for this flexibility was identified as an out-of-plane bending motion. The nature of this bending is shown in Figure 6, which shows schematically a side view of PBO as the out-of-plane bend angle increases from 0 to 15°. Clearly, the force constants governing such deformation are critically important in the MD simulations and the validity of the results depends on their accuracy.

Previous results<sup>3</sup> for the neutral molecules showed that the molecular mechanics force field gave higher energies associated with this out-of-plane bending than did either semiempirical (AM1) or *ab initio* calculations. Whether protonation of the molecules would increase these deformation energies remained unanswered. Figure 7 compares the AM1 energy curves associated with this bending for neutral and protonated molecules. All energies are plotted relative to the energies for the unbent, coplanar molecule having the same charge. Calculations were made for the bend occurring at the apex atoms of the phenyl and heterocycle rings. For PBZT, starting torsion angles of 0 and 20° were examined. The geometries were fully optimized except for the constraints necessary to impose the desired out-of-plane bending.

In contrast to the dramatic effects on the torsion energy, the bending energy increases less steeply for the protonated molecules than for the neutral molecules. The addition of a second proton has less effect than the first. By comparing the 0 to 20° torsion results for PBZT, it can also be seen that the deformation energy apparently

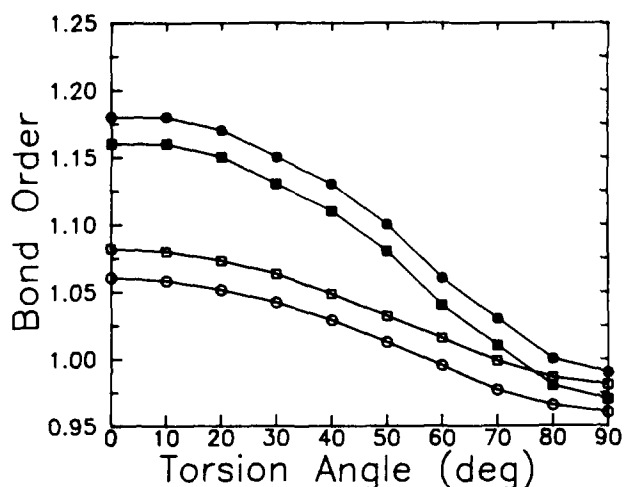


Figure 3 Bond order versus torsion angle for singly (open symbols) and doubly (filled symbols) protonated PBZT (circles) and PBO (squares). Protonation locations were the same as in Figure 2

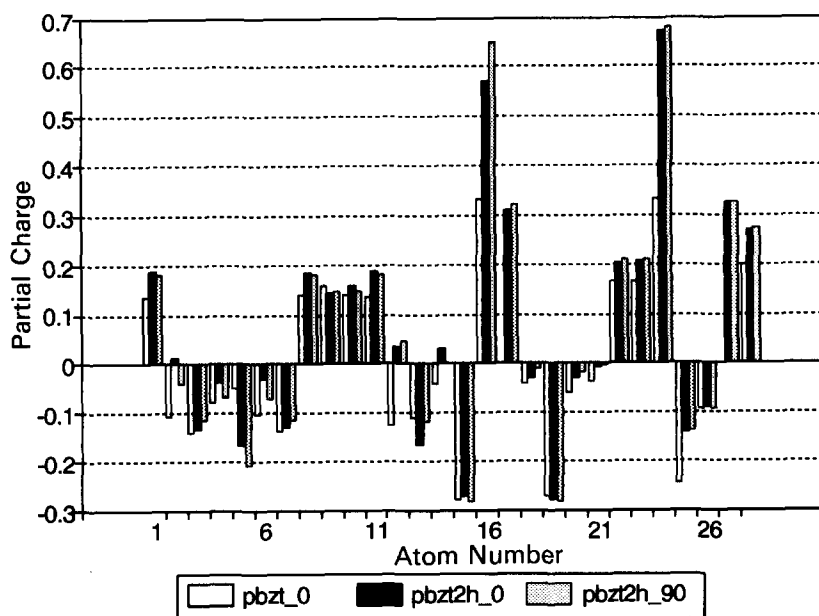
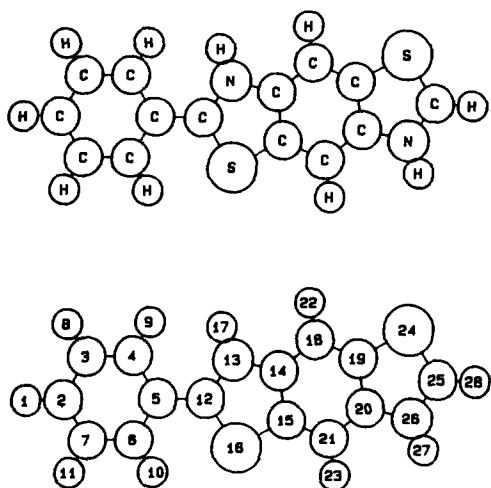
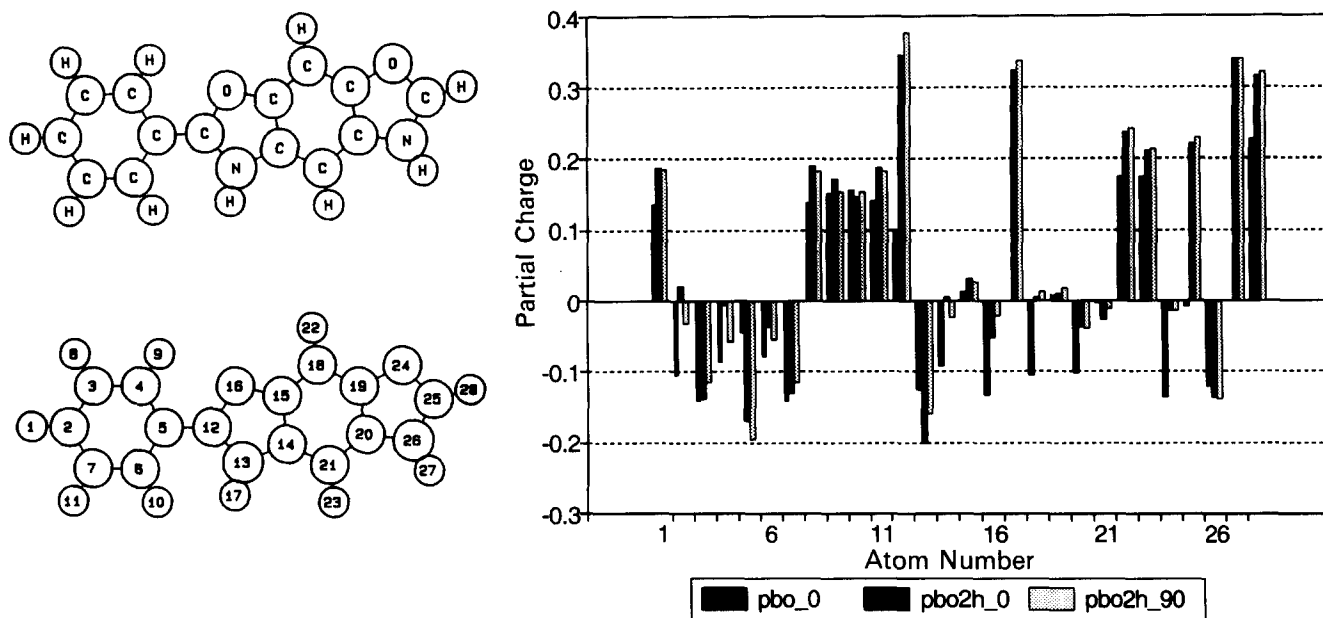


Figure 4 Comparison of charge distributions in neutral PBZT and doubly protonated PBZT at 0 and 90° torsion angles. Structural diagrams show the atom numbering scheme



**Figure 5** Comparison of charge distributions in neutral PBO and doubly protonated PBO at 0 and 90° torsion angles. Structural diagrams show the atom numbering scheme



**Figure 6** Side view of PBO molecule showing the mode of bending (0, 5, 10, and 15°) used for analysis of the deformation energy

does not change with torsion angle, at least for these small bend angles and near the coplanar conformation where such effects would be expected to be largest.

It appears that the force constants in the modified Tripos force field<sup>14</sup> used in the earlier MD simulations<sup>3</sup> would tend to overestimate the stiffness of the molecule even compared with their behaviour when protonated in solution. Preliminary MD calculations of protonated PBZT and PBO oligomers *in vacuo* suggest that intramolecular Coulombic interactions tend to increase the stiffness, though not dramatically. Shielding effects in a solvent would most probably leave the molecular stiffness not much greater than that *in vacuo*. Certainly, based on the present results, protonation does not have the effect of stiffening resistance to out-of-plane bending through alteration of the internal force constants. Neutral PBO and PBZT polymers were seen (in MD simulations) to adopt conformations having three-dimensional character<sup>3</sup>. In protonating solvents, on the other hand, this retained bendability, combined with the increased torsional energy barrier, suggests that the rigid-rod polymers may adopt more ribbon-like geometries, with the chain axis being more confined to a plane normal to that of the rings themselves.

Rigid-rod polymers complexed with Lewis acids can be dissolved in aprotic organic solvents, such as nitroalkanes and nitrobenzene<sup>9</sup>. The complexes are neutral and result from association of the Lewis acid with specific heteroatom (N or O) donor sites. Why are the complexes soluble and what does their solubility say about molecular stiffness? A polymer might dissolve

because of very strong interactions with the solvent. However, since the polymer–Lewis acid complexes are neutral, their interaction with an organic solvent would not be expected to be much different from that of the uncomplexed polymer. The primary role of the Lewis acid then might be taken to be disruption of the crystalline lattice of the polymer, thereby reducing the enthalpy of solution of the complex compared to that of the untreated polymer. In order that the material dissolves, the entropy of dissolution must now overcome only this reduced enthalpy. The mixing contribution to the entropy, however, is small in polymers. Thus, it seems likely that in order for the rigid-rod complexes to dissolve, there must be another contribution to the entropy. On the basis of MD simulations, this contribution appears to be that arising from conformational flexibility – that is, bending deformations coupled with torsional freedom. Further, the Lewis acid complexes with the heteroatoms of the polymer would not change the conformational properties of the polymer itself. For example, the  $\text{BF}_3$  group is sterically not much larger than a pendent methyl group. Thus, it can be inferred that not only the complexed rods, but the untreated rigid-rod polymers as well, must have significant conformational flexibility in solution. This is clearly consistent with the results of MD simulations<sup>3</sup> and the observed persistence lengths<sup>1,2</sup>.

#### *Ab initio calculations of ring opening*

According to the AM1 calculations, protonation of PBO at the nitrogen atom would be preferred energetically (by about  $2.4 \text{ kcal mol}^{-1}$ ) to protonation at the oxygen atom. The results also suggest, however, that protonation at the oxygen atom (should it actually occur first) would lead to breaking the bond between the oxygen and apex carbon atom, and thus to ring opening. Since ring opening is apparently not observed experimentally, *ab initio* calculations were undertaken to see if they also indicated ring opening upon protonation of the oxygen atom, and to verify that protonation at the nitrogen was in fact energetically preferable to protonation of the oxygen. Several oxazole and thiazole fragments which

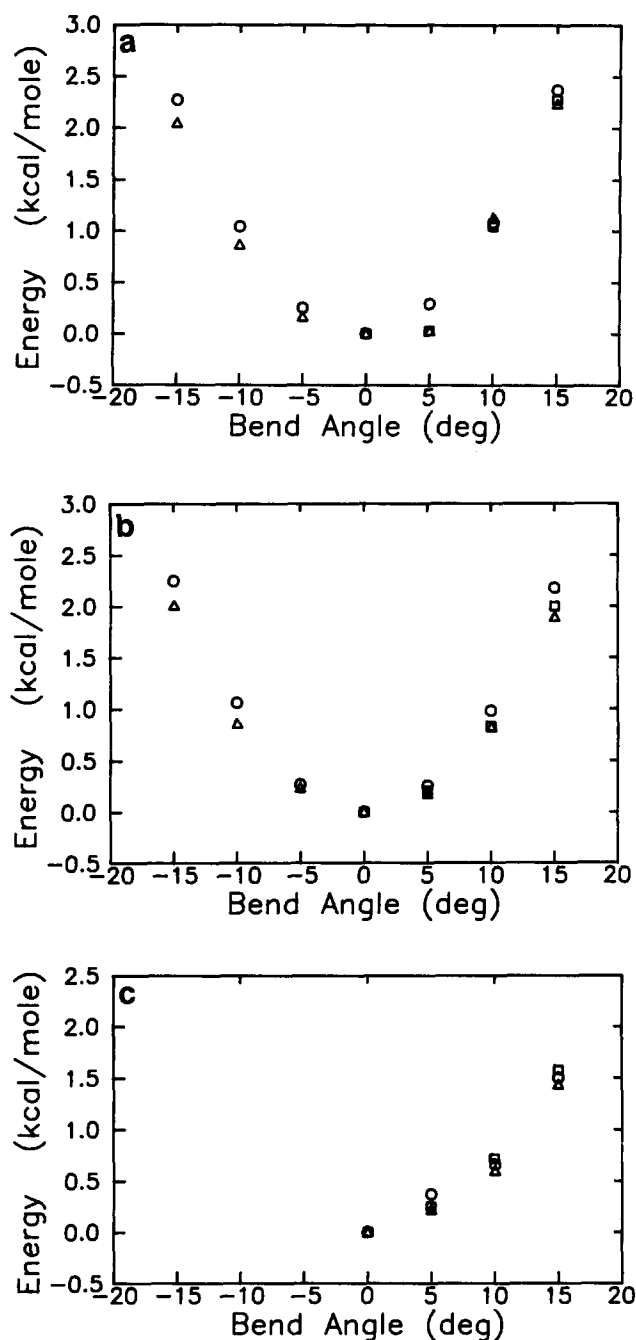


Figure 7 Energy versus bend angle for (a) PBO, (b) PBZT at 0° torsion angle and (c) PBZT at 20° torsion angle. Symbols and protonation sites are the same as for Figure 2

would be expected to behave in a manner similar to the relevant portion of the heterocycle, yet small enough to consider at *ab initio* levels, were studied. These are shown in Figure 8. Their energies, the computational methods used, and the basis sets used are shown in Table 2. Default optimization criteria and minimization procedures were used in every case.

Unlike the AM1 results on PBO, *ab initio* geometry optimization at the RHF/3-21G\* level did not lead to ring opening in the process of locating the minimum energy geometry. However, this appears to reflect a difference in the optimization procedures used or the nature of the potential energy surface explored by the two methods, rather than truly different predictions of the properties upon protonation. By comparing the energies of structures III and IV, it is clear that the opened

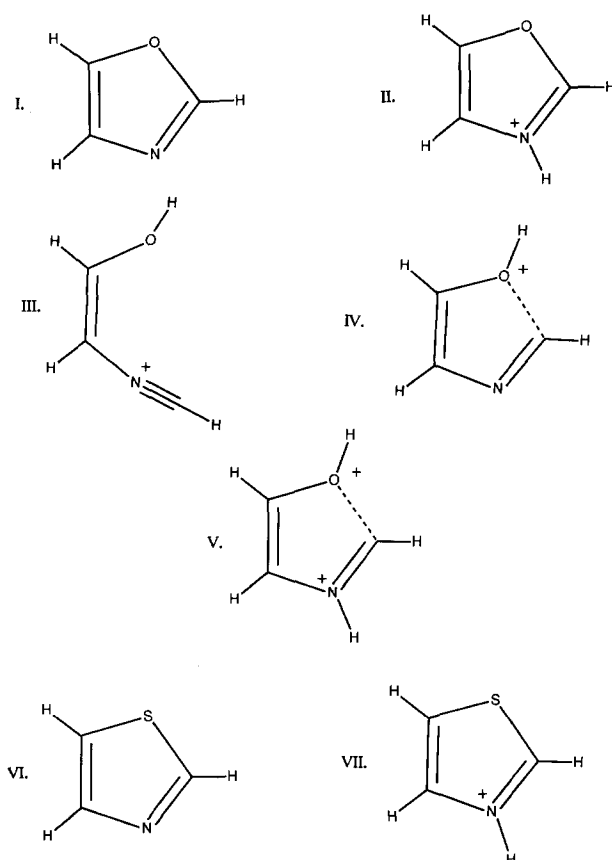


Figure 8 Structures of the molecular fragments used for determining protonation effects on ring stability. Dashed lines denote imposed constraints

Table 2 Characteristics of oxazole and thiazole fragments

Molecule	AM1	Heat of formation (Hartrees) <sup>a</sup>		
		RHF/3-21G*	RHF/6-31G**	MP2/6-31G**
PBO				
I	0.0197	-243.2511	-244.6387	
II	0.2735	-243.6145	-244.9963	-244.9925
III	0.2824	-243.5679	-244.9438	-244.9379
IV	(0.3711) <sup>b</sup>	-243.5322		
V	0.8211	-243.6825		
PBZT				
VI	0.0766	-564.4858		
VII	0.3267	-564.8597		

<sup>a</sup>1 Hartree = 627.5 kcal mol<sup>-1</sup>

<sup>b</sup>Constrained geometry

form has a lower energy (by about 22 kcal mol<sup>-1</sup>) than the closed ring with a protonated oxygen, in qualitative agreement with the AM1 result. (Quantitative comparison is not possible because the AM1 optimization did not locate a stable point for structure IV unless the C-O distance was artificially constrained. As shown in the table, such a constraint led to a very high energy. Without the constraint, the geometry transformed to that of structure III with the AM1 energy shown in the table for that structure.)

In order of increasing energies, the AM1 results and the more sophisticated *ab initio* methods rank the various structural fragments similarly. Calculations using AM1 parameterization for the fragments indicate protonation on the nitrogen (in the closed ring) is about 5.6 kcal mol<sup>-1</sup> lower in energy than protonation on the oxygen (in an

opened ring). The *ab initio* method likewise indicates that protonation should occur at the nitrogen. The energy difference between structure II and structure III is 29.3 kcal mol<sup>-1</sup> at the 3-21G\* level and 34.3 kcal mol<sup>-1</sup> at the MP2 level. With this considerably larger energy difference than indicated by AM1, the *ab initio* results do not support the likelihood of ring opening.

The influence of the phenyl ring on the possible reaction has not been considered explicitly in the *ab initio* calculations. However, the *ab initio* energies of fragments II, III and IV are in the same order as the results of the calculations on the full PBO repeat unit. Further, the AM1 optimization on the fragment led to ring opening, just as when the phenyl group was present. Given this overall similarity in results, it seems unlikely that inclusion of the phenyl ring would alter the *ab initio* results significantly in regard to the likelihood of ring opening in PBO.

The stability of the ring during optimization by *ab initio* methods is apparently consistent with the results of a study<sup>20</sup> of proton affinities in oxazole and thiazole. That study, using Gaussian 86 and a 6-31G basis set, made no mention of ring opening when the oxygen of oxazole was protonated. The authors did not consider protonation at the nitrogen atoms in either molecule. Our results indicate that protonation at the nitrogen is preferable to protonation of the oxygen or sulfur. Proton affinities of 224 and 234 kcal mol<sup>-1</sup> are found for oxazole and thiazole, respectively, based on energies using the 3-21G\* basis set. These values are comparable to that reported<sup>20</sup> for the imidazole ring – 246 or 239 kcal mol<sup>-1</sup> using 6-31G or 6-31G\* basis sets. From the energies in Table 2, energy differences of 3–5 kcal mol<sup>-1</sup> might be expected in going from the 3-21G\* to the higher basis sets. Thus it seems that even allowing for change in basis set, the proton affinities of oxazole and thiazole are very similar to that of imidazole rather than being 80 to 120 kcal mol<sup>-1</sup> less<sup>20</sup>.

The ring opening observed during AM1 optimization may be associated with the longer oxygen bond lengths (0.03–0.04 Å greater than calculated by *ab initio* methods) and 'singularly high values' of the heat of fusion of oxazole reported in a recent comparison<sup>21</sup> of AM1 and other semiempirical and *ab initio* methods. This may indicate an underestimation of the C–O bond strengths in the AM1 parameterization, which sufficiently modifies the potential energy surface to lead to bond cleavage upon protonation of the oxygen.

## CONCLUSIONS

The effects of protonation on the behaviour of PBO and PBZT repeat units have been examined. It was found that a significant portion of the charge deposited on the molecules was delocalized into the phenyl ring when it was coplanar with the heterocycle. The delocalization diminished as the torsion angle increased, with the result that the torsional energy barrier became substantially higher for the protonated molecules. In contrast, the resistance to out-of-plane bending deformation decreased slightly upon protonation. Thus, the flexibility observed in previous MD simulations of the neutral molecules *in vacuo* appears to be a reasonable depiction of the stiffness of the polymer even in strong acid solution.

## REFERENCES

- 1 Kumar, S. in 'International Encyclopedia of Composites' (Ed. S. M. Lu), Vol. 4, VCH, New York, 1990, pp. 51–74
- 2 Lee, C. C., Chu, S. G. and Berry, G. C. *J. Polym. Sci., Polym. Phys. Edn* 1983, **21**, 1573
- 3 Farmer, B. L., Chapman, B. R., Dudis, D. S. and Adams, W. W. *Polymer* 1993, **34**, 1588
- 4 Farmer, B. L., Chagin, T., Dudis, D. S. and Adams, W. W. 'Proc. 8th Int. Conf. on Deformation, Yield and Fracture of Polymers, Cambridge, UK', 1991, no. 107
- 5 Zhang, R. and Mattice, W. L. *Macromolecules* 1992, **25**, 4937
- 6 Green, K., Eby, R. K., Klunzinger, P. E., Farmer, B. L., Adams, W. W. and Czornyj, G. 'Proc. Soc. Plastics Engineers', ANTEC, 1991, **37**, 1532
- 7 Socci, E. P., Farmer, B. L. and Adams, W. W. *J. Polym. Sci., Polym. Phys. Edn* 1993, **31**, 1975
- 8 MacTurk, K., Eby, R. K. and Farmer, B. L. *Polymer* 1994, **35**, 53
- 9 Jenekhe, S. A., Johnson, P. O. and Agrawal, A. K. *Macromolecules* 1989, **22**, 3216
- 10 Stewart, J. J. P. MOPAC, QCPE Program no. 455
- 11 See articles in: *Macromolecules* 1981, **14**, 909–960
- 12 Adams, W. W., Eby, R. K. and McLemore, D. E. (Eds) 'The Materials Science and Engineering of Rigid-Rod Polymers', *Mater. Res. Soc. Symp. Proc.* 1989, **134**
- 13 Sybyl, Version 5.3, Tripos Associates, St Louis, MO
- 14 Clark, M., Cramer, R. D. III and Van Opdenbosch, N. *J. Comp. Chem.* 1989, **10**, 982
- 15 Farmer, B. L., Wierschke, S. G. and Adams, W. W. *Polymer* 1990, **31**, 1637
- 16 Farmer, B. L., Wierschke, S. G. and Adams, W. W. *Mater. Res. Soc. Symp. Proc.* 1989, **134**, 447
- 17 Wierschke, S. G. *Mater. Res. Soc. Symp. Proc.* 1989, **134**, 653
- 18 Gaussian 88, Frisch, M. J., Head-Gordon, M., Schlegel, H. B., Raghavachari, K., Binkley, J. S., Gonzalez, C. *et al.*, Gaussian, Inc. Pittsburgh, PA, 1986
- 19 Welsh, W. J. and Mark, J. E. *Polym. Eng. Sci.* 1983, **23**, 140
- 20 Kabir, S. and Sapse, A.-M. *J. Comp. Chem.* 1991, **12**, 1142
- 21 Shaffer, A. A. and Wierschke, S. G. *J. Comp. Chem.* 1993, **14**, 75